AUT Journal of Mechanical Engineering

AUT J. Mech. Eng., 4(1) (2020) 41-50
DOI: 10.22060/ajme.2019.14684.5738

Geometry Shape Effects of Nanoparticles on Fluid Heat Transfer Through Porous Channel

A. T. Akinshilo

Mechanical Engineering Department; University of Lagos, Akoka-Yaba, Nigeria

ABSTRACT: In this paper the geometry effects of different nanoparticles such as cylindrical, spherical and lamina on heat transfer of fluid transported through contracting or expanding micro channel are considered. The nanofluid flow and heat transfer through the porous channel are described using mathematical models. Since the mathematical models are nonlinear in nature the homotopy perturbation method, an approximate analytical method is adopted to provide solution to the mathematical model. The fast convergence rate coupled with analytical procedural stability motivates the use of the homotopy perturbation method as the favored method in providing solutions to the system of coupled, higher order differentials.The obtained analytical solution is used to investigate the influence of particle shape of the nano sized materials on heat transfer of fluid flowing through a porous medium considering a uniform magnetic field. It is illustrated from results that lamina nanoparticle shape shows higher dimensionless temperature and thermal conductivity when compared with nano shaped particles of cylinder and sphere respectively due to variations in thermal boundary layers. Results obtained from this study prove useful in the advancement of science and technology including micro mixing, nanofluidics and energy conservation. Comparing obtained analytical solution with fourth order numerical solution, good agreement was established.

Review History:

Received: 4 Jul. 2018
Revised: 10 Feb. 2019
Accepted: 10 Feb. 2019
Available Online: 11 Feb. 2019

Keywords:

Heat transfer
Nanofluid
Porous channel
Magnetic field
Homotopy perturbation method

1- Introduction

The significance attached to fluid heat transfer in modern times cannot be over emphasized. This is as a result of increasing energy pricing associated with fluid transportation. Since energy pricing plays an important role in the transport phenomena, it therefore becomes imperative to determine best ways of conserve fluid energy during transport. As it has tremendous importance in applications including but not limited to polymer processing, power plant operations and oil recovery applications. Upon this, heat transfer of fluid through porous micro channel as received wide considerations by engineers and scientist [1-15].

In recent times, research effort to study natural convective flows through porous channels was presented by Kargar and Akbarzade [1] using analytical methods. Pourmehran et al. [2] investigated the effect of micro channel heat sink on nanofluid to optimize thermal performance. Blood flow containing nanoparticles through porous arterial segment was analyzed by Ghasemi et al. [3] in the presence of magnetic field. Micropolar heat transfer and flow in permeable channel walls was presented by Fakour et al. [4] using analytical methods. Hatami and Jing [5] optimized mixed convective heat transfer in T shaped porous cavity. Flow through circular conduit using least square method was presented by Ghasemi [6] considering electro hydrodynamics. Hatami et al. [7] analyzed motion of spherical particles in plane coquette fluid flow adopting differential transform method.

*Corresponding author's email: ta.akinshilo@gmail.com

Natural convection flow in circular wavy cavity containing nanoparticles was studied by Hatami et al. [8] to optimize heat transfer. Shortly after Hatami and Ganji [9] extended their research to motion of spherical particles on rotating parabola adopting analytical techniques. Natural convective heat transfer of nanofluid flow through double sinusoidal walls was investigated by Tang and Jing [10] considering various phase deviations. Asymmetric porous channel heat transfer and flow of nanofluid was studied by Hatami et al. [11] using approximate analytical schemes.

Earlier works on the nanofluid study was performed by Choi [12]. The purpose of his research was to improve the transport and energy capacity of base fluids. Therefore he proposed the inclusion of nanometer sized metallic particles in base fluids such as grease, water and ethylene. It was discovered that fluid thermal conductivity as improved to about three times its initial state. Upon this other researchers have built upon [13-18]. Due to its relevance in practical modern science such as biomedicine, fuel cells and manufacturing. However since thickness of thermal boundary layer is influenced by nanoparticles shapes owing to simultaneous effect of density and thermal conductivity. The need to investigate nanoparticle shapes effect on working fluids becomes important [19,20]. Effect of size and surface chemistry of nanoparticle shapes was studied Albanese et al. [21] on biological systems. Geometrical description of metallic nanoparticles was presented by Rodriguez-Lopez et al. [22]. Jo et al. [23] investigated therapeutic effect of nanoparticles size, surface charge and shapes on brain and

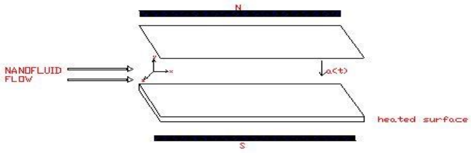

Fig. 1. Physical model of problem

retinal diseases.

The heat transfer of the engine oil base fluid containing various shapes of alumina nano sized particles is described by ordinary and nonlinear differentials of the higher order. Therefore it is required to adopt either numerical or analytical methods to generate solutions to the system of coupled equation. Hence analytical and numerical methods have been utilized by researchers in solving nonlinear problems in science and engineering [19-31].

The current paper therefore investigates the heat transfer effect of nano sized particle shapes of lamina, cylindrical and spherical considering an expanding or contracting flow channel with externally heated bottom plate. Utilizing the Homotopy Perturbation Method (HPM).

2- Model Development and Analytical Solution

The nanofluid considered is a mixture of engine oil and alumina. The fluid flows unsteadily through horizontally arranged parallel plates under the effect of applied magnetic field as described in the physical model diagram, Fig. 1. Component of velocity in the x and y direction is taking as u and v respectively. The upper plate contracts and expands at a uniform rate while the bottom plate is externally heated and fixed. Following the assumptions that the nano mixture is thermodynamically compatible, incompressible fluid flow since flow is in liquid phase only and negligible radiation effect due to flow geometry. Since fluid is viscous the Navier-Stokes equation is presented as Akinshilo [13]:

$$\frac{d^4 f}{d\eta^4}+\frac{A_1}{A_2}\left(\begin{array}{c}\alpha\left(\eta\frac{d^3 f}{d\eta^3}+3\frac{d^2 f}{d\eta^2}\right)+\\ R\left(f\frac{d^3 f}{d\eta^3}-\frac{df}{d\eta}\frac{d^2 f}{d\eta^2}\right)\end{array}\right)-M^2\frac{d^2 f}{d\eta^2}=0 \quad (1)$$

$$\begin{aligned}&\frac{d^2 q_m}{d\eta^2}-\frac{A_3}{A_4}PrRmq_m\frac{df}{d\eta}+\frac{A_3}{A_4}PrRf\frac{dq_m}{d\eta}\\&+\frac{A_3}{A_4}\alpha Prmq_m+\frac{A_3}{A_4}Pr\eta\alpha\frac{dq_m}{d\eta}\end{aligned} \quad (2)$$

With appropriate boundary condition introduced as

$$f(0)=0 \quad \frac{df}{d\eta}(0)=0 \quad f(1)=1 \quad \frac{df}{d\eta}(1)=1 \quad (3)$$

$$q_m(0)=1, q_m(1)=0 \quad (4)$$

The effect of expansion or contraction on the fluid is measured by α, applied magnetic field intensity is predicted by the Hartmann parameter M, the influence of momentum diffusivity against thermal diffusivity is determined by the Prandtl number represented as Pr. The significance of inertia compared to viscous fluid is measured by the Reynolds number depicted as R.

Nanofluid constant parameters are stated as:

$$A_1=\frac{\rho_{nf}}{\rho_f},\quad A_2=\frac{\mu_{nf}}{\mu_f} \quad (5)$$

$$A_3=\frac{\left(\rho C_p\right)_{nf}}{\left(\rho C_p\right)_f}, A_4=\frac{k_{nf}}{k_f} \quad (6)$$

where heat capacitance $\left(\rho C_p\right)_{nf}$, effective dyn amic viscosity $\left(\mu_{nf}\right)$, effective density (ρ_{nf}), thermal conductivity (k_{nf}) is represented as above. The nanoparticles shapes are considered following the model proposed by Hamilton and Crosser [19,20] defined as follows:

$$\rho_{nf}=\left(1-\phi\right)\rho_f+\phi\rho_s \quad (7)$$

$$\left(\rho C_p\right)_{nf}=(1-\phi)(\rho C_p)_f+\phi(\rho C_p)_s \quad (8)$$

$$\mu_{nf}=\frac{\mu_f}{(1-\phi)^{2.5}} \quad \text{(a)}$$

$$\frac{k_{nf}}{k_f}=\frac{k_s+(b-1)k_f-(b-1)\phi(k_f-k_s)}{k_s+(b-1)k_f-\phi(k_f-k_s)} \quad \text{(b)} \quad (9)$$

The empirical shape factor b, whose thermo physical properties are expressed in Table 1. According to Fig. 2 the ratio of the height (h) to diameter (d) is expresses as N. Hence the shape factor is represented as

$$(N)=\frac{2N+1}{2N}\sqrt[3]{12N} \quad (10\text{-a})$$

Where N for cylinder is defined as N≥10 and lamina as

Table 1. Thermo physical properties of nanofluid [31].

	Density (kg/m^3)	Specific heat capacity(J/kg.K)	Thermal conductivity (W/m.K)
Engine Oil	884	1910	0.144
Al_2O_3	3970	765	40

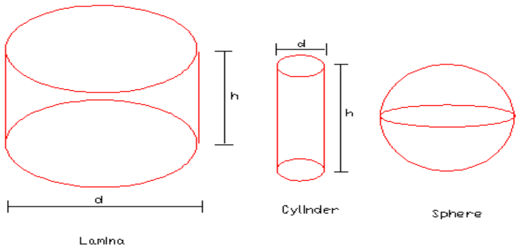

Fig. 2. Shapes for different nanoparticle type.

N$\leq$0.1. Its numerical values are given in Table 2. Similarly sphericity (φ) which is the ratio of the surface area of the sphere geometrical shape to the surface area of the real shape at the given volume. This is expressed as

$$\varphi(N)=\frac{2N}{2N+1}\sqrt[3]{\frac{9}{4N}} \tag{10-b}$$

With the numerical values given in Table 2.

2- 1- Application of the homotopy perturbation method

Geometry effect of nanoparticles on heat transfer of fluid transported through the channel is analyzed utilizing the homotopy perturbation method whose principles and fundamentals have been described thoroughly by Kargar and Akbarzade [1]. Therefore homotopy perturbation method, an approximate analytical solution is considered in this paper. The fast convergence rate coupled with analytical procedural stability motivates the use of the HPM as the favored method in providing solutions to the system of coupled, higher order differentials.Upon constructing the homotopy, the Eqs. (1) and (2) is expressed as:

Table 2. Values of empirical and shape factor for different nanoparticle shape.

	Sphere	Cylinder	Lamina
φ	1	0.4710	0.1857
b	3	6.3698	16.1576

$$H_1(p,\eta)=(1-p)\left[\frac{d^4f}{\partial\eta^4}\right]+ p\left[\begin{array}{l}\dfrac{d^4f}{d\eta^4}+\dfrac{A_1}{A_2}\left(\begin{array}{l}\alpha\left(\eta\dfrac{d^3f}{d\eta^3}+3\dfrac{d^2f}{d\eta^2}\right)\\ +R\left(f\dfrac{d^3f}{d\eta^3}-\dfrac{df}{d\eta}\dfrac{d^2f}{d\eta^2}\right)\end{array}\right)\\ -M^2\dfrac{d^2f}{d\eta^2}\end{array}\right]=0 \tag{11}$$

$$H_2(p,\eta)=(1-p)\left[\frac{d^2q_m}{d\eta^2}\right]+ p\left[\begin{array}{l}\dfrac{d^2q_m}{d\eta^2}-\dfrac{A_3}{A_4}PrRmq_m\dfrac{df}{d\eta}\\ +\dfrac{A_3}{A_4}PrRf\dfrac{dq_m}{d\eta}+\dfrac{A_3}{A_4}\alpha Prmq_m+\dfrac{A_3}{A_4}Pr\eta\alpha\dfrac{dq_m}{d\eta}\end{array}\right]=0 \tag{12}$$

Taking power series of velocity and temperature fields yields

$$\begin{aligned} f&=P^0f_0+P^1f_1+P^2f_2+....... &&\text{(a)}\\ q_m&=P^0q_{m0}+P^1q_{m1}+P^2q_{m2}+....... &&\text{(b)}\end{aligned} \tag{13}$$

Substituting Eq. (13-a) into Eq. (11) and selecting at the various order yields

$$p^0:\frac{d^4f_0}{d\eta^4} \tag{14}$$

$$p^1:\frac{d^4f_1}{d\eta^4}+\frac{A_1}{A_2}\alpha\eta\frac{d^3f_0}{d\eta^3}+3\frac{A_1}{A_2}\alpha\frac{d^2f_0}{d\eta^2} +\frac{A_1}{A_2}Rf_0\frac{d^3f_0}{d\eta^3}-\frac{A_1}{A_2}R\frac{df}{d\eta}\frac{d^2f_0}{d\eta^2}-M^2\frac{d^2f_0}{d\eta^2} \tag{15}$$

$$p^2:\frac{d^4f_2}{d\eta^4}+\frac{A_1}{A_2}\alpha\eta\frac{d^3f_1}{d\eta^3}+3\frac{A_1}{A_2}\alpha\frac{d^2f_1}{d\eta^2}+\frac{A_1}{A_2}Rf_0\frac{d^3f_1}{d\eta^3}+\frac{A_1}{A_2}Rf_1\frac{d^3f_0}{d\eta^3}-\frac{A_1}{A_2}R\frac{df_0}{d\eta}\frac{d^2f_1}{d\eta^2}-\frac{A_1}{A_2}R\frac{df_1}{d\eta}\frac{d^2f_0}{d\eta^2}-M^2\frac{d^2f_1}{d\eta^2} \tag{16}$$

Substituting Eq. (13-b) into Eq. (12) and selecting at the various order yields

$$p^0:\frac{d^2q_{m0}}{d\eta^2} \tag{17}$$

$$p^1:\frac{d^2q_{m1}}{d\eta^2}-\frac{A_3}{A_4}PrRmq_{m0}\frac{df_0}{d\eta}+\frac{A_3}{A_4}PrRf_0\frac{d^2q_{m0}}{d\eta}+\frac{A_3}{A_4}Pr\alpha mq_{m0}+\frac{A_3}{A_4}Pr\alpha\eta\frac{dq_{m0}}{d\eta} \tag{18}$$

$$p^2:\frac{d^2q_{m2}}{d\eta^2}-\frac{A_3}{A_4}PrRmq_{m0}\frac{df_1}{d\eta}-\frac{A_3}{A_4}PrRmq_{m1}\frac{df_0}{d\eta}+\frac{A_3}{A_4}PrRf_0\frac{d^2q_{m0}}{d\eta^2}+\frac{A_3}{A_4}PrRf_1\frac{d^2q_{m0}}{d\eta^2}+\frac{A_3}{A_4}Prmq_{m1}+\frac{A_3}{A_4}Pr\eta\alpha\frac{dq_1}{d\eta} \tag{19}$$

Leading order boundary condition is given as

$$f_0(0)=0\quad \frac{df_0}{d\eta}(0)=0\quad f_0(1)=1\quad \frac{df_0}{d\eta}(1)=1 \tag{20}$$

Simplifying Eq. (14) applying the leading order boundary condition Eq. (20) yields

$$f_0=\frac{3}{2}\eta^2-\frac{\eta^3}{2} \tag{21}$$

Leading order boundary condition is given as

$$q_{m0}(0)=1,q_{m0}(1)=0 \tag{22}$$

Simplifying Eq. (17) applying the leading order boundary condition Eq. (22) yields

$$q_{m0}=1-\eta \tag{23}$$

First order boundary condition is given as

$$f_1(0)=0\quad \frac{df_1}{d\eta}(0)=0\quad f_1(1)=1\quad \frac{df_1}{d\eta}(1)=1 \tag{24}$$

Simplifying Eq. (15) applying the first order boundary condition Eq. (24) yields

$$f_1=\frac{3A_1\alpha\eta^5}{120A_2}+\frac{9A_1\alpha\eta^5}{120A_2}-\frac{9A_1\alpha\eta^4}{48A_2}+\frac{9A_1\alpha\eta^6}{1440A_2}-\frac{3A_1R\eta^7}{1680A_2}+\frac{9A_1R\eta^7}{1680A_2}-\frac{27A_1R\eta^6}{1440A_2}+\frac{9A_1R\eta^5}{480A_2}-\frac{3M^2\eta^5}{120}+\frac{3M^2\eta^4}{48}-\frac{\eta^3}{6}\left[12-\frac{36A_1\alpha}{80A_2}+\frac{324A_1R}{2240A_2}+\frac{12M^2}{40}\right]-\frac{\eta^2}{2}\left[-6-\frac{A_1\alpha}{40A_2}-\frac{A_1R}{35A_2}-\frac{M^2}{40}\right] \tag{25}$$

First order boundary condition is given as

$$q_{m1}(0)=1,q_{m1}(1)=0 \tag{26}$$

Simplifying Eq. (18) applying the first order boundary condition Eq. (26) yields

$$q_{m1}=\frac{3A_3PrRm}{24A_4}\left(\eta-\eta^4\right)-\frac{3A_3PrRm}{40A_4}\left(\eta-\eta^5\right)-\frac{3A_3PrRm}{12A_4}\left(\eta-\eta^3\right)+\frac{3A_3PrRm}{24A_4}\left(\eta-\eta^4\right)+\frac{\alpha A_3Prm}{2A_4}\left(\eta-\eta^2\right)-\frac{\alpha A_3Prm}{6A_4}\left(\eta-\eta^3\right)-\frac{\alpha A_3Pr}{6A_4}\left(\eta-\eta^3\right) \tag{27}$$

The order two coefficients for $f(\eta)$ and $q_m(\eta)$ in Eqs. (16) and (19) were too voluminous to be mentioned here but are expressed graphically in the results and results validation, Table 3. Therefore final expressions for flow and heat transfer is expressed as

$$f(\eta)=f_0(\eta)+f_1(\eta)+f_2(\eta) \tag{28}$$

Table 3. Comparison of values of η for dimensionless temperature distribution. Where R=m=α=1, □=0.05, M= b=0.

η	$q(\eta)$ Numerical Solution	Present Study (HPM)	Error
0	1.0000	1.0000	0.0000
0.1	0.8937	0.8937	0.0000
0.2	0.7877	0.7877	0.0000
0.3	0.6824	0.6824	0.0000
0.4	0.5781	0.5781	0.0000
0.5	0.4754	0.4754	0.0000
0.6	0.3747	0.3747	0.0000
0.7	0.2765	0.2765	0.0000
0.8	0.1812	0.1812	0.0000
0.9	0.0889	0.0889	0.0000
1.0	0.0000	0.0000	0.0000

Table 4. Comparison of values of η for dimensionless temperature distribution for sphere, cylinder and lamina nanoparticles. Where R=m=α=1, □=0.05, Pr=0.2, M=0.

η	$q(\eta)$ Sphere	Cylinder	Lamina
0.2	0.7853	0.7854	0.7855
0.3	0.6783	0.6786	0.6787
0.4	0.5730	0.5734	0.5735
0.5	0.4700	0.4705	0.4706
0.6	0.3698	0.3702	0.3704
0.7	0.2725	0.2729	0.2731
0.75	0.2250	0.2254	0.2255
0.8	0.1784	0.1787	0.1788
0.85	0.1325	0.1328	0.1329

$$q_m(\eta) = q_{m0}(\eta) + q_{m1}(\eta) + q_{m2}(\eta) \tag{29}$$

Relevant phenomena with practical significance on heat and mass transfer can be reduced to the Nusselt number defined as

$$Nur = -A_4 q'_m(0) = -\frac{k_{nf}\partial T}{k_f \partial \eta} / (T_w - T_0) \tag{30}$$

3- Results and Discussion

In this section, graphical presentations are used to describe obtained analytical solutions as shown in Figs. 1 to 4. With the influence of nanoparticle shape geometry on heat transfer through the porous channel

discussed. The accuracy of the approximate analytical result obtained using the homotopy perturbation method is validated using numerical solution as shown in Table 3 for active parameters. Numerical solution is obtained using the Runge-Kutta-Fehlberg method whose accuracy has been improved through the addition of mid-point in the step which has been used as suitable method [4-6]. The effect of Reynolds parameter (R) on heat transfer is depicted in Fig. 3. As observed Fig. 3(a) depicts the effect of spherical shaped nanoparticles on heat transfer. It is seen that quantitative increase in R leads to decreasing temperature distribution which is significant towards the mid plate. The effect of cylindrical shaped nanoparticles on heat transfer as shown in Fig. 3(b) shows decreasing temperature distribution with higher R parameter though effect is more when compared with the sphere nanoparticles. Also the influence of the lamina shaped nanoparticle geometry is presented in Fig. 3(c) which depicts numeric increase in R parameter shows decreasing temperature distribution which is coherent with the sphere and cylindrical shape nanoparticles. This is due to decreasing thermal boundary layer thickness. However the lamina shaped nanoparticle present the highest temperature distribution amongst the three nanoparticle shapes adopted.

expansion ratio (α) causes increase in temperature distribution towards the bottom plate and as the upper plate is approached a slight decrease in temperature distribution is seen using the sphere shaped nanoparticles. Utilizing

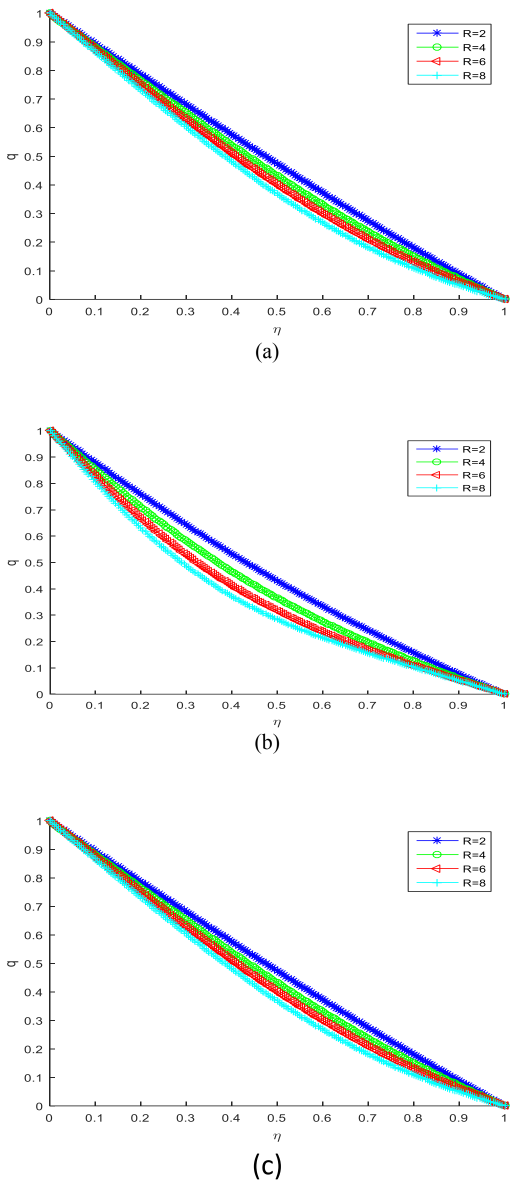

Fig. 3. Effect of Reynolds number on temperature profile (a) Sphere shaped nanoparticle. (b) Cylinder shaped nanoparticle. (c) Lamina shaped nanoparticle.

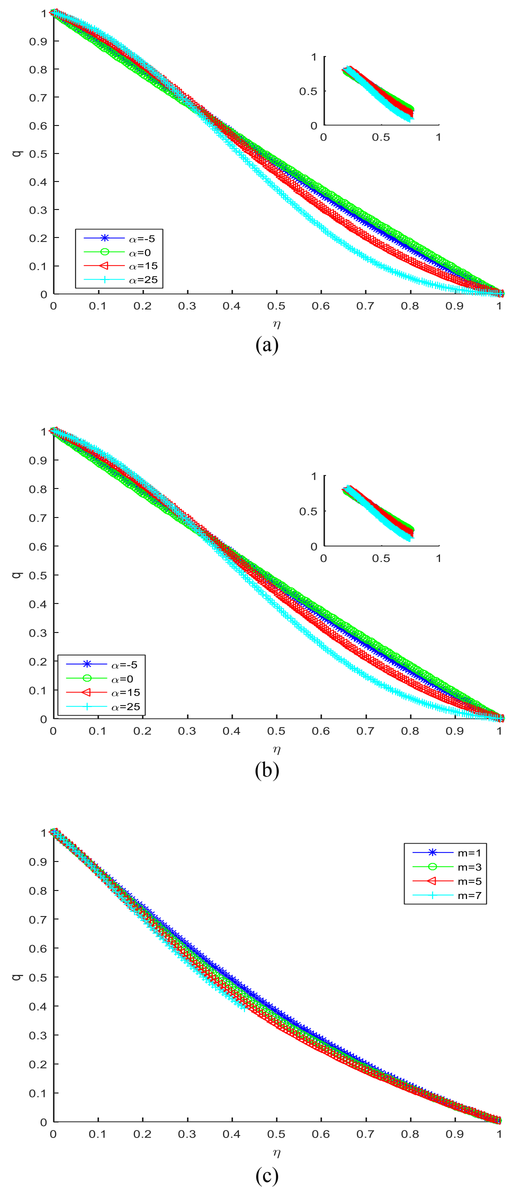

Fig. 4. Effect of expansion ratio on temperature profile (a) Sphere shaped nanoparticle. (b) Cylinder shaped nanoparticle. (c) Lamina shaped nanoparticle.

cylindrical shaped nanoparticles, heat transfer effect can be observed in Fig. 4(b) which shows similar trend with the sphere nano shaped particle. More so the lamina shaped nano particle predicts a slight increase in temperature profile with increasing α parameter towards the lower plate but around η=0.45 (not determined accurately) there is decrease in the temperature profile which is obvious towards the upper plate. Nano sized particles of lamina shape shows stronger thermal boundary layer thickness compared with cylindrical and spherical shapes respectively. This is physically explained as a result of increasing injection velocity variations.

Temperature index (m) effect on heat transfer of the nanofluid is observed in Fig. 5. As illustrated from Fig. 5(a), numeric increase in m parameter causes decrease in temperature distribution adopting the spherical nanoparticle but using the cylindrical shaped nanoparticle decreasing temperature distribution is also observed in Fig. 5(b). The temperature distribution of the cylindrical shaped nanoparticle is higher compared with the sphere shaped. Also utilizing the lamina shaped nanoparticle Fig. 5(c), decreasing temperature distribution is seen. Lamina shaped nano size particle predicts a lower rate of temperature decrease compared with the cylindrical and sphere nanoparticles as a result of wall temperature variations.

Nano particle concentration (□) effect on temperature distribution is represented by Fig. 6. As observed in Fig. 6(a) adopting the sphere shaped nanoparticle numeric increase of □ shows significant decrease in temperature profile across the plate, however towards the upper plate slight decrease in temperature distribution is demonstrated. This result is

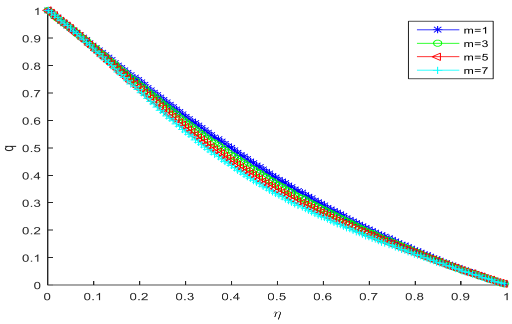

(a)

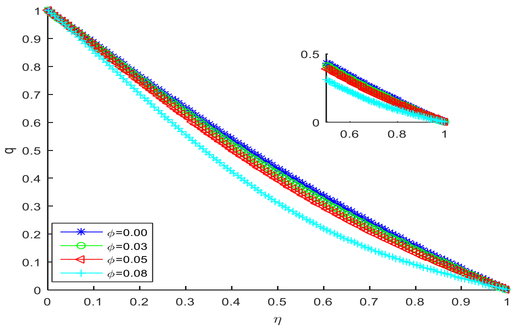

(b)

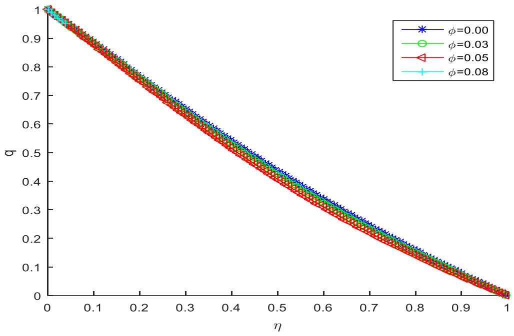

(c)

Fig. 5. Effect of temperature index on temperature distribution (a) Sphere shaped nanoparticle. (b) Cylinder shaped nanoparticle. (c) Lamina shaped nanoparticle.

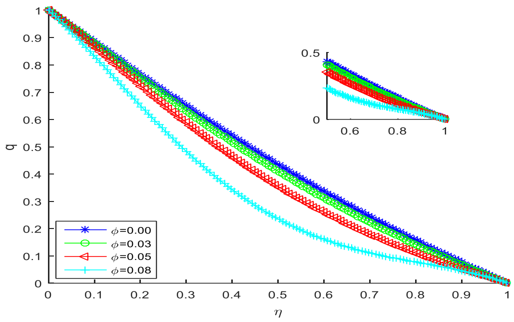

(a)

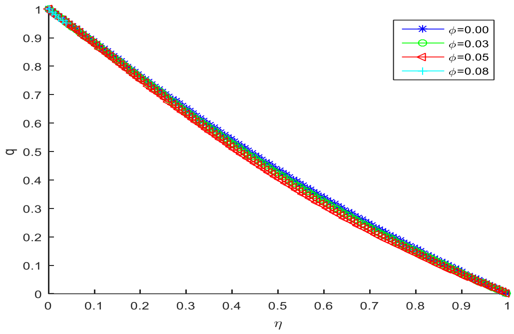

(b)

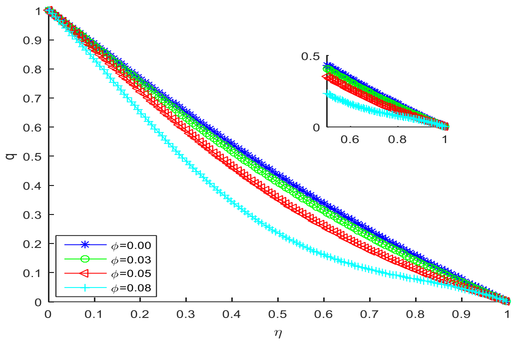

(c)

Fig. 6. Effect of nanoparticle concentration on temperature distribution (a) Sphere shaped nanoparticle. (b) Cylinder shaped nanoparticle. (c) Lamina shaped nanoparticle.

similar to the result obtained in Adnan et al. [31]. Effect of cylinder shaped nanoparticle is depicted in Fig. 6(b) where it is observed that increasing nanoparticle concentration effect shows concentration decrease across the flow channel. While nanoparticle concentration effect using lamina shaped nano sized particle is shown in Fig. 6(c). It is observed from the plot that increasing □ causes slight decrease in temperature distribution across the region of flow. This phenomenon can be explained physically due to high mass and heat transfer caused by increased thermal conductivity leading to increased thickness of thermal boundary layer. However should the nanoparticle be neglected from the fluid, effect is demonstrated as □=0.00. Increasing effect of nanoparticle concentration improves the thermal performance most especially the lamina shape then the cylinder and sphere shape respectively as depicted in Table 4. This is in good agreement with the conclusion obtained in Adnan et al. [31].

Influence on the nano shaped size particle can be observed from the Fig. 7. Though the effect is not too significant on the plots. However it can be depicted from the plots that as nano centration increases quantitatively heat transfer rate increases but towards the upper plate around η=0.7 (not accurately determined) a reverse trend is notice. The sphere nano shaped particle as the highest Nusselt number followed by the cylindrical shape. More so the lamina shape nanoparticle has the lowest Nusselt number, amongst the nano shaped sized particle under consideration.

4- Conclusion

The geometry effect of nanoparticles such as cylinder,

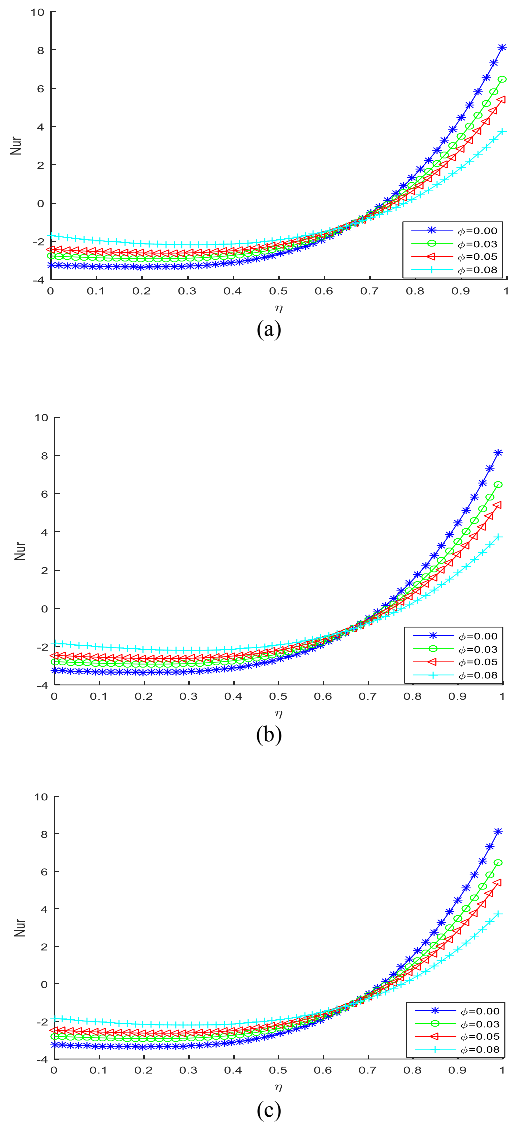

Fig. 7. Effect of nanoparticle concentration on Nusselt number using (a) Sphere shaped nanoparticle. (b) Cylinder shaped nanoparticle. (c) Lamina shaped nanoparticle.

lamina and sphere on heat transfer through porous channel is considered in this paper. Analyses of heat transfer of nano fluid through porous channel are performed adopting the homotopy perturbation method. Results obtained from the approximate analytical solutions due the fluid mechanics are used to investigate the effect of important fluid parameters on heat transfer. It is proven from analysis that the lamina shaped nanoparticles as a higher dimensionless temperature and thermal conductivity at the same fluid parameters compared with the cylinder and spherical shape respectively. Present study provides exciting insights to numerous engineering applications such as energy conservation, micro mixing and nano fluidics amongst others.

Conflict of Interest

The author declares no competing interest as regard paper publication.

Nomenclature

$f(\eta)$	Stream function variable
k	Thermal conductivity
M	Index of temperature
Nu	Nusselt number
R	Reynolds number
Pr	Prandtl number
T	Temperature
u	x velocity component
v	y velocity component
M	Hartmann parameter
Greek symbols	
α	Expansion ration
μ	Viscosity
ϕ	Nanoparticle concentration
ρ	Density
η	Non-dimensional y direction $[y/a]$
Subscript	
f	Fluid
nf	Nanofluid
s	Solid
w	Wall

References

[1] A. Kargar, M. Akbarzade, Analytical solution of natural convection flow of a non-Newtonian fluid between two vertical parallel plates using the Homotopy Perturbation Method, World Applied Science Journal 20 (2002) 1459-1465.

[2] O. Pourmehran, M. Rahimi-Gorji, M. Hatami, S.A.R. Sahebi, G. Domairry, Numerical optimization of microchannel heat sink (MCHS) performance cooled by KKL based nanofluids in saturated porous medium, Journal of the Taiwan Institute of Chemical Engineering 55(2015) 49-68

[3] S.E. Ghasemi, M. Hatami, A.K. Sarokalaine, D.D. Ganji, Study on blood flow containing nanoparticles through porous arteries in presence of magnetic field using analytical methods, Physica E: Low-dimensional System and Nanostructures 70 (2015) 146-156.

[4] M. Fakour, A. Vahabzadeh, D.D. Ganji, M. Hatami, Analytical study of micropolar fluid flow and heat transfer in a channel with permeable walls, Journal of Molecular Liquids 204(2015) 198-204.

[5] M. Hatami, D. Jing, Optimization of a lid-driven T-shaped porous cavity to improve the nanofluids mixed convection heat transfer, Journal of Molecular Liquids 231(2017) 620-631.

[6] S.E. Ghasemi, M. Hatami, G.H.R. Mehdizadeh Ahangar, D.D. Ganji, Electro hydrodynamic flow analysis in a circular cylindrical conduit using least square method, Journal of Electrostatics 72(2014) 47-52.

[7] M. Hatami, M.Sheikholeslami, G.Domairry, High accuracy analysis for motion of a spherical particle

in plane Couette fluid flow by Multi-step Differential Transformation Method, Powder Technology 260(2014) 59-67.

[8] M. Hatami, D. Song, D.D. Jing, Optimization of a circular-wavy cavity filled by nanofluid under the natural convection heat transfer condition, International Journal of Heat and Mass Transfer 98 (2016) 758-767.

[9] M. Hatami, D.D. Ganji, Motion of a spherical particle on a rotating parabola using Lagrangian and high accuracy multi-step differential transformation method, Powder Technology 258 (2014) 94-98.

[10] W. Tang, D. Jing, Natural convection heat transfer in a nanofluid-filled cavity with double sinusoidal wavy walls of various phase deviations, International Journal of Heat and Mass Transfer 115 (2017) 430-440.

[11] M. Hatami, M. Sheikholeslami, D.D. Ganji, Nanofluid flow and heat transfer in an asymmetric porous channel with expanding or contracting wall, J. of Molecular Liquids 195 (2014) 230-239.

[12] S.U.S. Choi, Engineering thermal conductivity of fluids with nanoparticles, Development and Application of Non-Newtonian Flows 66 (1995) 99-105.

[13] A.T. Akinshilo, Flow and heat transfer of nanofluid with injection through an expanding or contracting porous channel under magnetic force field, Engineering Science and Technology, an International Journal 21 (2018) 486-494.

[14] M.G. Sobamowo, A.T. Akinshilo, On the analysis of squeezing flow of nanofluid between two parallel plates under the influence of magnetic field, Alexandria Engineering Journal 57 (2018) 1413-1423.

[15] W.A. Khan, A. Aziz, Double diffusive natural convection boundary layer flow in a porous medium saturated with a nanofluid over a vertical plate, prescribed surface heat, solute and nanofluid fluxes, International Journal of Thermal Science 50 (2011) 2154-2160.

[16] W.A. Khan, A. Aziz, Natural convective boundary layer flow over a vertical plate with uniform surface heat flux, International Journal of Thermal Science 50 (2011) 1207-1217.

[17] A.T. Akinshilo, J.O. Olofinkua, O. Olaye, Flow and Heat Transfer Analysis of Sodium Alginate Conveying Copper Nanoparticles between Two Parallel Plates, Journal of Applied and Computational Mechanics 3 (2017) 258-266.

[18] M.R. Hashimi, T. Hayat, A. Alsaedi, On the analytic solutions for squeezing flow of nanofluids between parallel disks, Nonlinear Analysis Modeling and Control 17(4) (2014) 418-430.

[19] M. Sheikholeslami, M.K. Sadoughi, Mesocopic method for MHD nanofluid flow inside a porous cavity considering various shapes of nanoparticles, International Journal of Heat and Mass Transfer 113 (2017) 106-114.

[20] E. Sourtiji, M. Gorji-Bandpy, D.D. Ganji, S.F. Hosseinizadeh, Numerical analysis of mixed convective heat transfer of Al2O3-water nanofluid in a ventilated cavity considering different positions of the outlet port, Powder Technology 262 (2014) 71-81.

[21] A. Albanese, P.S. Tang, W.C.W. Chan, The effect of nanoparticle size, shape and surface chemistry on biological systems, A. Reviews of Biomedical Engineering 14 (1) (2012) 1-16.

[22] J.L. Rodriguez-Lopez, J.M. Montejano-Carrizales, J.P. Palomares-Baez, M.J. Yacamas, Size effect and shapes stability of nanoparticles, Key Engineering Material 444(2010) 47-68.

[23] D.H. Jo, J.H. Kim, T.G. Lee, J.H. Kim, Size, surface charge and shape determine therapeutic effects of nanoparticles on brain and retinal diseases, Nanomedication: Nanotechnology Biology and Medicine 11 (7) (2015) 1603-1611.

[24] M. Sheikholeslami, M.M. Rashidi, D.M. Alsaad, F. Firouzi, H.B. Rokni, G. Domairry, Steady nanofluid flow between parallel plates considering thermophoresis and Brownian effect, Journal of King Saud University - Engineering Science 49 (4) (2015) 6-15.

[25] A.A. Joneidi, D.D. Ganji, M. Babaelah, Differential transform method to determine fin efficiency of convective straight fins with temperature dependent thermal conductivity, International Communication in Heat and Mass Transfer 39 (2009) 757-762.

[26]. Filobello-Niño,H. Vazquez-Leal, K. Boubaker, Y. Khan, A. Perez-Sesma, A. Sarmiento Reyes, V.M. Jimenez-Fernandez,A. Diaz-Sanchez, A., Herrera-May, J. Sanchez-Orea, K. Pereyra-Castro, Perturbation Method as a Powerful Tool to Solve Highly Nonlinear Problems: The Case of Gelfand's Equation, Asian Journal of Mathematics and Statistics 3(2) (2013) 76-82.

[27] M. Hatami, Nanoparticles migration around the heated cylinder during the RSM optimization of a wavy-wall enclosure, Advanced Powder Technologgy 28 (2017) 890-899.

[28] Z. Ziabakhsh, G. Domairry, Analytic solution of natural convection flow of a non-Newtonian fluid between two vertical flat plates using homotopy analysis method, Communication Nonlinear Science Numumerical Simulation 14 (2009) 1868-1880.

[29] A. Mehmood, A. Ali, Analytic solution of three dimensional viscous flow and heat transfer over a stretching surface by homotopy analysis method, American Society of Mechanical Engineers 130 (2008) 21701-21707.

[30] H.A. Hoshyar, D.D. Ganji, A.R. Borranc, M. Falahatid, Flow behavior of unsteady incompressible Newtonian fluid flow between two parallel plates via homotopy analysis method, Latin American Journal of Solids and structures 12 (2015) 1859-1869.

[31]. Filobello-Niño,H. Vazquez-Leal, K. Boubaker, Y. Khan, A. Perez-Sesma, A. Sarmiento Reyes, V.M. Jimenez-Fernandez,A. Diaz-Sanchez, A., Herrera-May, J. Sanchez-Orea, K. Pereyra-Castro, Perturbation Method as a Powerful Tool to Solve Highly Nonlinear Problems: The Case of Gelfand's Equation, Asian Journal of Mathematics and Statistics 3(2) (2013) 76-82.